Molecular Dynamics Simulation of Epitaxial Growth

Ivan K. Schuller

Reprinted from Materials Research Society
MRS Bulletin, Volume XIII,
Number 11, November 1988.

Molecular Dynamics Simulation of Epitaxial Growth

Ivan K. Schuller

Introduction

The growth of thin films has been instrumental in the study of many areas of material science, physics, metallurgy, and chemistry and is an important ingredient in the development of many devices.[1] Although experimental studies have been extensively pursued for many years, theoretical studies have only been performed using model calculations which rely on a number of unknown parameters *a priori*. Only recently have attempts been made to understand thin film growth using real-time numerical simulation.[2,3] The main reason for the recent increase of such studies is the development of computers capable of tackling a problem of the magnitude required to understand thin film growth. The phenomena present in thin film growth occur for systems containing many particles (e.g., columnar growth) and long relaxation times, which strain the capabilities presently available in modern supercomputers. Further increases in computational power might bring a number of important problems within reach and improve our understanding of thin film growth at the microscopic level.

I will present a number of epitaxial growth studies we have performed using molecular dynamics (MD) techniques. I will show that a number of properties predicted by these calculations are in good agreement with experimental observations. These include the microcrystalline and epitaxial growth of metal films, the growth of amorphous films in mixtures of metals, and the vapor phase growth of silicon. Finally, I will outline several important studies yet to be implemented.

The technique described here for the simulation of growth from the vapor phase involves a full MD simulation of the problem.[4] In these calculations, given an interatomic potential and a procedure for controlling temperature, the classical equations of motion of the whole system are solved simultaneously without further approximations. The weakness of the method resides in the availability of "correct" interatomic potentials. This is especially true for epitaxial growth where an atom approaches a free surface. Although a technique developed quite recently allows recalculating the interatomic potentials at every MD step,[5] the computational capabilities required prohibit applying this method to epitaxial growth. Moreover, as I will show, a number of important and interesting properties can be studied without such sophisticated methods.

Potentials and Epitaxy

To simulate metals it is customary to use *spherically symmetric* potentials such as the Lennard-Jones (LJ) or Morse potentials.[6] In some cases the potential parameters are determined by a detailed fit to a bulk property such as the elastic constants. Since many other MD studies have been performed using LJ potentials, most studies of epitaxial growth have also been done using this same potential. Moreover, the general conclusions drawn from these studies rely *only* on the fact that the LJ potential consists of a hard-core repulsive core, an attractive part, and spherical symmetry. The LJ potential is given by:

$$V(r) = 4\varepsilon[(\sigma/r)^{12} - (\sigma/r)^{6}] \quad (1)$$

with the units of length and energy given by σ and ε respectively. The integration time step is typically taken to be $\Delta t = 0.02 t_o$ in the usual LJ units $t_o = (m\sigma^2/\varepsilon)^{1/2}$, with m being the particle mass. To simulate a mixture of two particles we have only varied the sizes (σ_i) and kept constant the depth of the potential.

Semiconductors, on the other hand, require more complex potentials such as the *fourfold coordinated* Stillinger-Weber potential,[7] which consists of two body parts of LJ type:

$$f_2(r_{ij}) = A(B r_{ij}^{-p} - 1) \exp[(r_{ij} - a)^{-1}] \quad (2)$$

and three body parts

$$f_3(r_{ij}, r_{ik}, \theta_{jik})\lambda \exp[\gamma(r_{ij} - a)^{-1} + \gamma(r_{ik} - a)^{-1}] [\cos\theta_{jik} + 1/3]^2 \quad (3)$$

with $A = 7.049556$, $B = 0.6022246$, $p = 4$, $a = 1.80$, $\lambda = 21.0$, and $\gamma = 1.20$.

It is important to stress that the conclusions drawn at present from such simulations are only qualitative and should not be applied to specific systems (e.g., a particular element).

Spherically Symmetric Potentials: Metals

Spherically symmetric potentials are expected to give a reasonable, qualitative idea for the physics of metal epitaxy. A more precise description of the physics of metals would require the use of volume-dependent potentials[8] or of the new combined density-functional-molecular-dynamics technique developed by Car and Parinello.[5] With the present understanding of epitaxial growth, a number of interesting conclusions can be drawn without the addition of such complications. Moreover, many interesting phenomena (e.g., "columnar growth") require studying large numbers of particles, making the use of more complicated schemes prohibitive.

Homoepitaxy ("like on like" growth) reveals a number of interesting phenomena in qualitative agreement with experimental observations.[9] Figure 1 shows the particle density along the z axis (perpendicular to the substrate) after the deposition of 2,052 atoms at a substrate temperature $T_s = 0$. The arrangement of atoms in the layers is shown in Figure 2. Even at very low temperatures, the growth is into defected *layered, microcrystalline* structures — as is observed in most metals — with the exception of Bi and Sb.[10] The small displacements required to move atoms into their equilibrium positions are supplied by the dynamics and the energy of the incoming particles. These are assumed to have Gaussian velocity distribution corresponding to a beam with an effective temperature of 0.9 (melting temperature of an LJ crystal ~0.7), as is

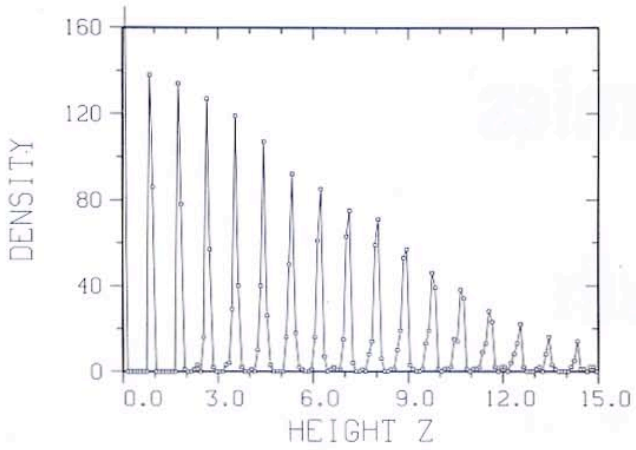

Figure 1. Particle density as a function of height for Lennard- Jones particles (metals) at $T_s = 0$. Note the presence of distinct layers with increasingly less particles at higher levels.

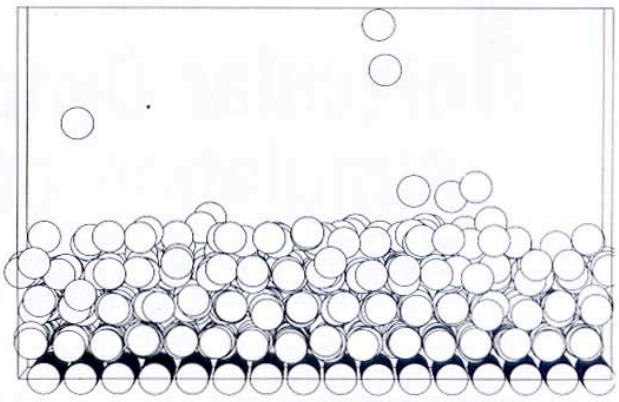

Figure 3. Layer-by-layer growth at $T_s = 0.4$.

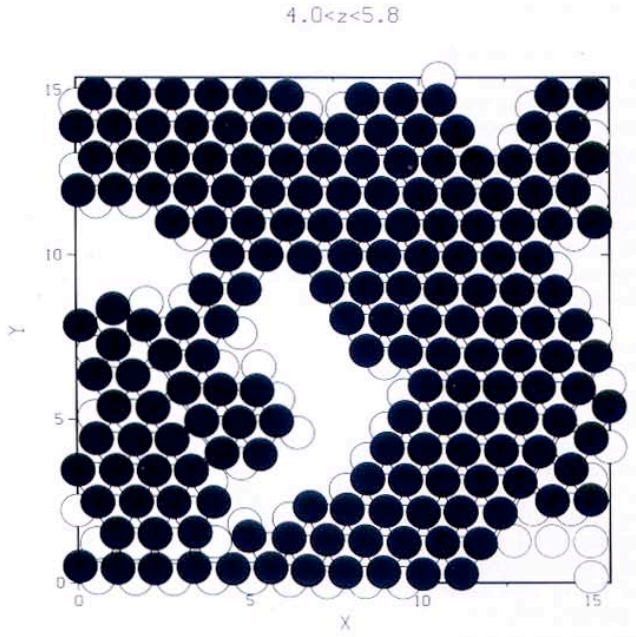

Figure 2. Two atomic layers stacked upon each other showing hexagonal patches and incomplete layers at $T_s = 0$.

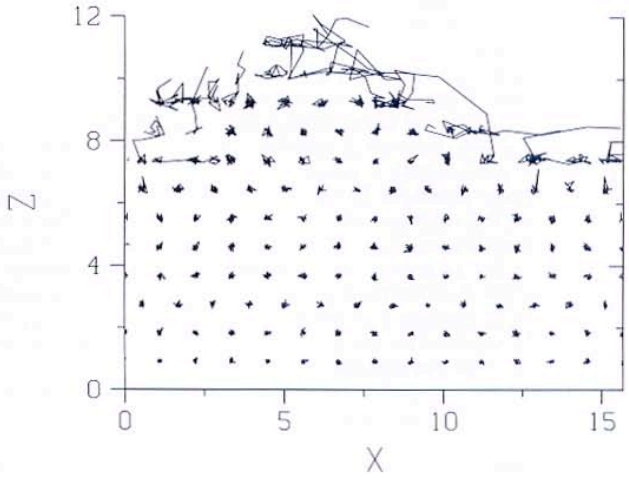

Figure 4. Particle trajectories followed for 1,500 molecular dynamics steps after the deposition of the last particle.

typical in metal epitaxy experiments. The spherical symmetry of the potential makes the growth of *amorphous* layers more difficult, and therefore the absence of mono-atomic amorphous metals is due to the symmetry of the potential, which allows the various atoms to "slide" around each other. However, big holes are present which increase in size as the height from the substrate increases. This implies that the layers are incomplete and the growth does not proceed in a layer-by-layer fashion.

Growth at high temperatures ($T_s \simeq$ 0.4), corresponding to epitaxial growth, is quite different. In this case, a "side view" of the growing film (Figure 3) shows that all the layers are completed and no holes are left. The growth proceeds layer by layer and can be quantified more precisely by a plot of particle density in each layer as a function of time.[9] The reason for the layer completion is that atoms on the surface are considerably mobile. The exchange of particles is observed four to five monolayers from the growing front (see Figure 4) by the trajectory of particles followed for about 200 ps.

Notice that atoms can move consider-

able distances. This implies that interfaces between two elements that have similar atomic radii would be interdiffused for about 4–5 atomic planes. Most systems that have lattice-matched crystal structures also have similar ionic radii and form solid solutions in their binary thermodynamic phase diagrams.[11] It has been shown that layer-by-layer growth requires temperatures close to half the melting temperature, and therefore the growth of atomically sharp interfaces in systems that have similar atomic radii (lattice matched, solid solutions in binary phase diagram) is difficult. Experimental observation of such systems require invoking unusual growth kinetics limitations and/or the presence of some yet unknown mechanism which keeps interfaces atomically sharp and flat.

Mixtures of Spherically Symmetric Potentials: Amorphous Metals

Amorphous growth of spherically symmetric potentials requires using a mixture of at least two different potentials. The reason, as with homoepitaxy, is that the growth dynamics, together with the symmetry of the potential, produces a microcrystalline structure at all temperatures. One possibility for a simplified calculation[12] is to use two "particle sizes" — σ_{AA} and σ_{BB} — but keep the depth of the potential constant. The length parameter for unlike particles is given by the simplest choice: $\sigma_{AB} = (\sigma_{AA} + \sigma_{BB})/2$. To understand the role of the different parameters, the two types of particles are introduced alternately, each having a Gaussian velocity distribution corresponding to a beam temperature of 0.9 (with the melting temperature of a Lennard-Jones crystal at ~0.7).

Above a ratio of $\sigma_{AA}/\sigma_{BB} > 0.9$, the growth again proceeds into well defined layers, with crystalline growth at all temperatures. However, for $\sigma_{AA}/\sigma_{BB} < 0.9$ the growth becomes considerably more disordered. For instance, Figure 5 shows the atomic density as a function of height z from the substrate for $\sigma_{BB}/\sigma_{AA} = 0.875$. After about five atomic layers from the substrate, the growth ceases to be in well-defined layers, i.e., all heights become equally populated. A picture of the atomic positions in a slice parallel to the x-y plane also reflects this disorder (Figure 6). Clearly the size ratio is an important parameter which controls growth in a crucial way.

All calculations show that an abrupt change occurs in the growth mode at a critical value of $\sigma_{BB}/\sigma_{AA} = 0.89 \pm 0.01$, at an epitaxy temperature $T_s = 0.4$. Figure 7 shows the number of distinct layers as a function of σ_{BB}/σ_{AA} at $T_s = 0.4$. The number of distinct crystalline layers diverges at the critical ratio — contrary to what one might naively expect. The physical reason for this abrupt transition is not well understood. It has been suggested that the crystalline-disordered transition occurs for a ratio for which dense packing differing by one particle (between the small and big sizes) is attained.

The present result corroborates the well-known empirical rule for the size effect, which states that "the atomic radii of two elements must differ by more than 10% for their binary alloys to form a glass."[13,14] Although the fundamental origin of this rule has not been identified, clearly the present results imply that the physical origin of this rule is possibly geometric, as suggested earlier.[14]

Coordinated Potentials: Semiconductors

As described earlier, the main difference distinguishing "metals" and "semiconductors" is the coordination implied by the potential. While the physical properties of metals are reasonably well simulated by spherically symmetric potentials, simulation of the properties of semiconductors requires using potentials which imply a well defined coordination. For instance, many of the physical properties of silicon have been reasonably well adjusted using the Stillinger-Weber[7] potential (Eqs. 2 and 3). As a first approach toward understanding the epitaxial growth of semiconductors, we performed a variety of studies using this potential. The results are distinct from

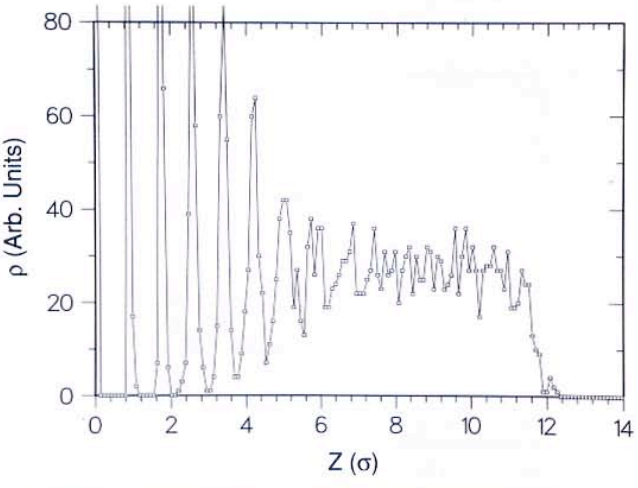

Figure 5. Particle density as a function of height from the substrate for a size ratio σBB/σAA = 0.875. Notice that after a few well-developed layers, all heights become equally populated. The height is measured in atomic units of the larger atoms.

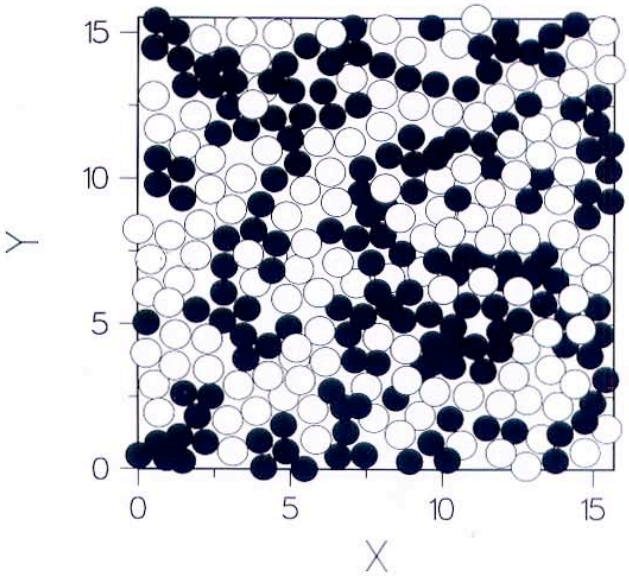

Figure 6. In-plane structure for the film shown in Figure 5.

those obtained using spherically symmetric potentials.[15,16]

Figure 8 shows the particle density along the growth (z) direction at a low substrate temperature $T_s = 0$. Beyond approximately two to three layers from the substrate, all heights are equally populated, indicating a disordered growth. The x-y plane atomic arrangement clearly reflects this (see Figure 9); no crystalline patches are observable. This is in qualitative agreement with experimental results, i.e., the growth of silicon at low substrate temperature is amorphous. The main reason for this type of growth seems to arise from the lowest atomic mobility existent with this type of potential.

Growth at intermediate substrate temperatures, however, is quite different. For instance, well-defined layered growth in the proper stacking sequence (AaBbCcAa . . .) is observed for intermediate substrate temperatures (Figure 10). However, considerable defects are observed which tend to become worse as the deposit becomes thicker. In general, these studies show that the growth is critically controlled by the potential, whereas the exact tempera-

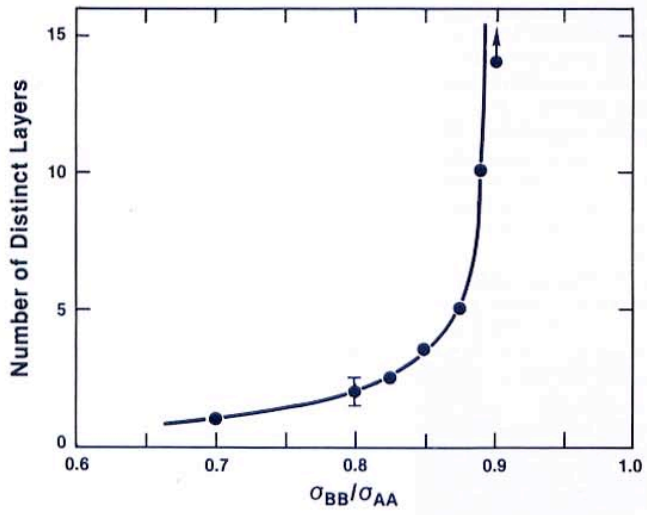

Figure 7. Number of distinct layers as a function of size ratio σBB/σAA (substrate layers excluded).

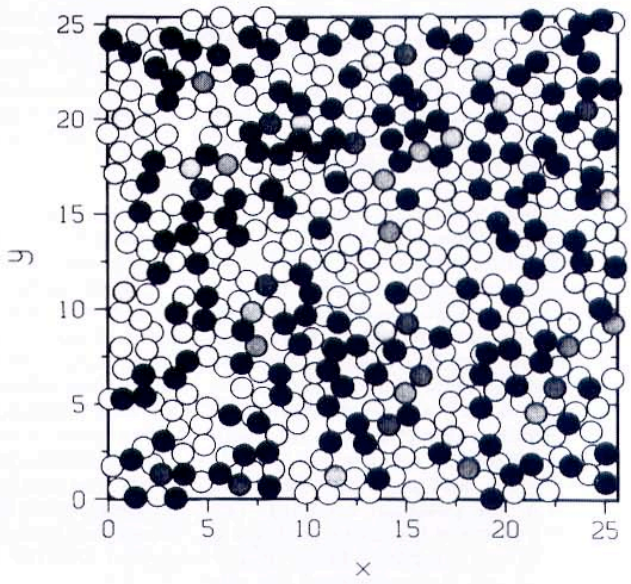

Figure 9. Atomic arrangement in a horizontal slice parallel to the substrate. Different gray shades correspond to different z values. Note the presence of a large number of rings.

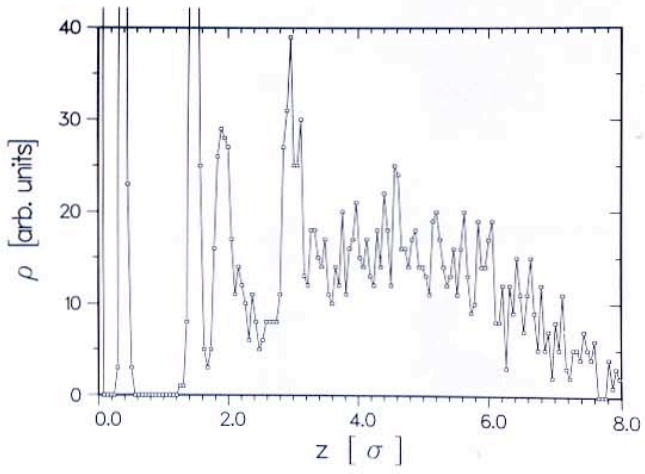

Figure 8. Particle density in the perpendicular direction for Stillinger-Weber (Si) particles at $T_s = 0$.

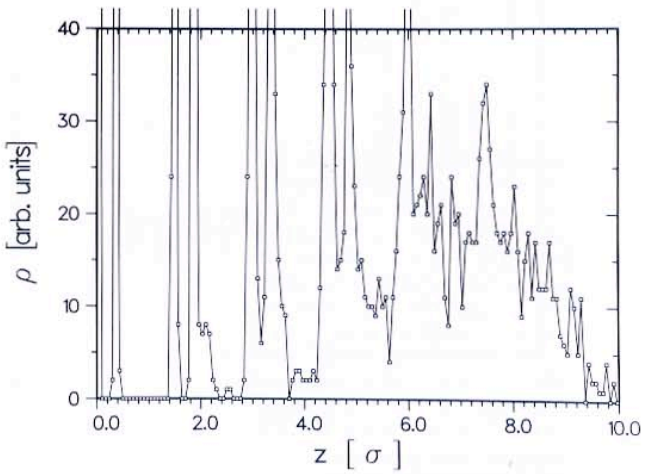

Figure 10. Atomic density in the perpendicular direction showing the formation of well-defined layers at intermediate temperatures.

ture doesn't play a precise role as long as it is "low enough" or "high enough" for a particular type of growth.

Conclusions

Molecular dynamics simulation has been used to study the growth of crystalline or amorphous, metal, and semiconductor films. These simulations show that the general form of the potential is critical in determining the morphology of vapor-phase grown films, with temperature playing a less important role. The high mobility of particles on the growing front implies that thermodynamics, together with kinetics, is important for thin film growth.

Future Studies

Clearly the recent molecular-dynamics simulations have only scratched the surface of the vast area of epitaxial growth. Many more studies are needed in order to ascertain the role of the relevant physical parameters in the growth. Questions related to the role of the energy distribution of incoming particles (thermal vapor deposition vs. sputtering), growth of metals on substrates which are not closed packed; heteroepitaxy under a variety of conditions; multilayered growth, etc., are only a few of the problems which molecular dynamics may address using currently available computational capabilities.

A number of other studies including realistic evaporation rates, columnar growth, and thick vs. thin film epitaxy, are straining or are beyond currently available computational capabilities. Using unconventional display forms such as motion pictures, developing novel computational schemes and tricks, and developing special purpose and/or new computational architectures such as parallel computing bring many of the problems mentioned above closer to reality. Of course, many of the ideas outlined here might benefit from a strong interaction with laboratory studies and may expand into other branches of computational physics.

Acknowledgments

This paper is dedicated to the memory of Prof. Aneesur Rahman, who has helped so many of us to take our first steps in the field of molecular dynamics. Many thanks to my collaborator, M. Schneider, with whom I enjoyed many hours of fascinating discussions. This work was partially supported by the National Science Foundation under Grant No. DMR 87-01921.

References

1. See for instance, *Epitaxial Growth*, edited by J.W. Matthews, (Academic Press, New York, 1975).
2. See for instance, M. Baskes, M. Daw, B. Dodson, and S. Foiles, *MRS Bulletin* **13** (2) (1988) p. 28.
3. See for instance, *Interfaces, Superlattices and Thin Films*, edited by J.D. Dow and I.K. Schuller (Mater. Res. Soc. Symp. Proc. **77**, Pittsburgh, PA, 1987).
4. A. Rahman, *Phys. Rev.* **136** (1964) p. A405.
5. R. Car and M. Parinello, *Phys. Rev. Lett.* **55** (1985) p. 2471.
6. H.J. Leamy, G.H. Gilmer, and A.G. Dirks in *Current Topics in Materials Science*, Vol. 6, edited by E. Kaldis (North-Holland, Amsterdam, 1980) p. 309.
7. F.H. Stillinger and T.A. Weber, *Phys. Rev. B* **31** (1985) p. 5262.
8. M.S. Daw and M.I. Baskes, *Phys. Rev. B* **29** (1984) p. 6443.
9. M. Schneider, A. Rahman, and I.K. Schuller, *Phys. Rev. Lett.* **55** (1985) p. 604.
10. W. Buckel and R. Hilsch, *Z. Phys.* **138** (1954) p. 109.
11. See for instance, M. Hansen, *Constitution of Binary Alloys* (McGraw-Hill Co., New York, 1958) and supplements.
12. M. Schneider, A. Rahman and I.K. Schuller, *Phys. Rev. B* **34** (1986) p. 1643.
13. See for instance, B.C. Giessen in *Proc. 4th Int. Conf. on Rapidly Quenched Metals*, Vol. 1, edited by T. Masumoto and K. Suzuki (Japan Inst. Metals, Sendai, 1982) p. 213.
14. T. Egami and Y. Waseda, *J. Non-Cryst. Sol.* **64** (1984) p. 113.
15. M. Schneider, I.K. Schuller, and A. Rahman, *Phys. Rev. B* **36** (1987) p. 1340.
16. R. Biswas, G.S. Grest, and C.M. Soukoulis, *Phys. Rev. B* (in press). □